ISTITUTO NAZIONALE DI FISICA NUCLEARE
Laboratori Nazionali di Frascati

LNF-85/62

A. Nakamura, L. Satta:
THE TENSOR ANALYZING POWER IN BACKWARD pd ELASTIC SCATTERING AND ITS RELATION TO $pp \rightarrow \pi d$ AT INTERMEDIATE ENERGIES

Estratto da:
Nuclear Phys. A445, p.706(1985)

Servizio Documentazione
dei Laboratori Nazionali di Frascati
Cas. Postale 13 - Frascati (Roma)

Nuclear Physics A445 (1985) 706–716

THE TENSOR ANALYZING POWER IN BACKWARD pd ELASTIC SCATTERING AND ITS RELATION TO $pp \to \pi d$ AT INTERMEDIATE ENERGIES

A. NAKAMURA*

Institute for Nuclear Study, University of Tokyo, Tanashi, Tokyo 188, Japan

L. SATTA

INFN - Laboratori Nazionali di Frascati, PO Box 13, 00044 Frascati, Italy

Received 21 February 1985
(Revised 26 April 1985)

Abstract: The tensor analyzing power for pd backward elastic scattering is calculated in the energy range $150 \leq T_p \leq 800$ MeV. Two main contributions are considered: the one-nucleon-exchange and the so-called triangle graph, including $pp \to \pi d$ as a subprocess. The pd backward elastic cross section and tensor analyzing power are fairly well reproduced by the model.

1. Introduction

Backward pd elastic scattering has been the subject of extensive work, experimental and theoretical, for nearly fifteen years. The excitation function at 180° is now rather well known up to incident proton kinetic energies of $T_p = 2.7$ GeV. It exhibits a monotonous decrease with increasing energy, broken by two structures: the first is centered around $T_p \simeq 0.5$ GeV, and the second, not yet completely explored, begins at $T_p \simeq 2.3$ GeV [refs. [1-5])].

The mechanisms involved in the interpretation of the first of these structures can be roughly classified into three categories:

(i) a one-pion exchange, with virtual $\Delta(1232)$ production in the intermediate state [6-9]);

(ii) a shoulder of the deuteron form factor in a Glauber-type model [10]);

(iii) a three-nucleon resonance in the s-channel [11]).

All these models reproduce the gross features of the backward cross section. A method to discriminate among them is to look at the tensor analyzing power, whose energy dependence, as pointed out by Vasan [12]), should be sensitive to the microscopic structure of the model.

The T_{20} measurements at backward angles and for energies $0.15 \leq T_p \leq 1.2$ GeV recently published [18]), show that the analyzing tensor attains large negative values,

* Fujukai Foundation fellow.

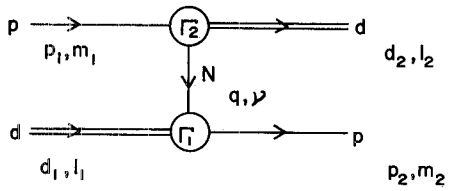

Fig. 1. The one-nucleon-exchange graph for pd → dp.

and its energy trend is richly structured. These measurements are in marked disagreement with earlier ones [13]), where T_{20} is compatible with zero in the same energy range. Theoretical predictions [14]) do not adequately describe these new results.

In this paper we propose an interpretation of the backward tensor analyzing power and cross section in terms of a model in category (i).

We shall assume that the elastic proton–deuteron backward scattering amplitude is made up of two contributions: (i) the one-nucleon-exchange mechanism (ONE), fig. 1; (ii) the triangle diagram including pp → πd as a subprocess, fig. 2.

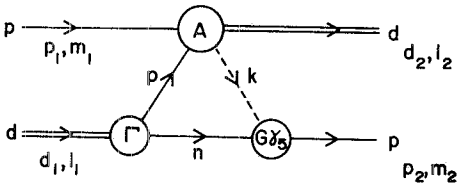

Fig. 2. The one-pion-exchange (triangle) diagram for dp → dp.

The ONE is the most elementary process for the backward scattering. At high energies, however, the momentum transfer in the u-channel is far from the one-nucleon pole and we should take into account the other contributions which are represented by the diagram in fig. 3. In the rest frame of the initial deuteron, the exchanged nucleon is "slow" and the following picture emerges: the incident proton hits one of the nucleons inside the target deuteron; together they form a deuteron moving forward with the emission of a pion which is absorbed by the other nucleon inside the target deuteron.

This triangle mechanism was proposed, as far as we know, by Craigie and Wilkin [6]). Later Kolybasov and Smorodinskaya [7]) pointed out that an approximation employed in the paper by Craigie and Wilkin is too rough, and leads to a wrong result.

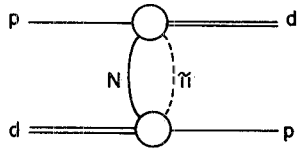

Fig. 3. Nπ exchange in the u-channel. The triangle graph is a special case of this diagram.

Unfortunately, their calculation includes several mistakes and they introduced a certain factor for the ONE diagram to get the best agreement with experiment.

Starting from these pioneer papers, we will formulate the calculation of amplitudes corresponding to figs. 1 and 2, and analyze the experimental data for the cross section and the tensor analyzing power.

2. Scattering amplitudes

As discussed in sect. 1, we include the triangle diagram as well as the ONE. Spin amplitudes are, therefore, written as

$$F^{m_2 l_2}_{m_1 l_1} = M^{m_2 l_2}_{m_1 l_1} + T^{m_2 l_2}_{m_1 l_1}, \tag{1}$$

where the M's are ONE amplitudes and the T's triangle mechanism contributions. Spin states of the incident proton, the outgoing proton, the initial deuteron and the final deuteron are denoted by m_1, m_2, l_1 and l_2. We quantize all spins along the direction of the initial momentum. These amplitudes are normalized as

$$\frac{\mathrm{d}\sigma}{\mathrm{d}\Omega_{\mathrm{c.m.}}} = \frac{(2m)^2}{64\pi^2 S}\frac{1}{6}\sum_{\mathrm{spin}}|F|^2, \tag{2}$$

i.e. they are invariant amplitudes. Here m is the proton mass.

The thirty-six spin amplitudes are not independent. For the backward scattering ($\theta = \pi$) which we will investigate in this paper, they are related to each other by parity conservation as

$$\begin{aligned} &T^{\frac{1}{2}\,1}_{\frac{1}{2}\,1} = a, \quad T^{-\frac{1}{2}-1}_{-\frac{1}{2}-1} = -a, \quad T^{\frac{1}{2}\,0}_{\frac{1}{2}\,0} = b, \quad T^{-\frac{1}{2}\,0}_{-\frac{1}{2}\,0} = -b, \\ &T^{\frac{1}{2}\,0}_{-\frac{1}{2}\,1} = c, \quad T^{-\frac{1}{2}\,0}_{\frac{1}{2}-1} = -c, \quad T^{-\frac{1}{2}\,1}_{\frac{1}{2}\,0} = c', \quad T^{\frac{1}{2}-1}_{-\frac{1}{2}\,0} = -c', \\ &T^{-\frac{1}{2}\,1}_{-\frac{1}{2}\,1} = d, \quad T^{\frac{1}{2}-1}_{\frac{1}{2}-1} = -d. \end{aligned} \tag{3}$$

Furthermore time-reversal invariance requires

$$c = c'. \tag{4}$$

2.1. ONE-NUCLEON EXCHANGE

We follow the procedure by Vasan [12]) and Anjos *et al.* [9]) to construct a ONE amplitude, but in order to clarify their contribution to the reaction we will give here the full expression. We use the notation of Bjorken and Drell [15]).

The Feynman amplitude corresponding to fig. 1 is

$$M = \bar{u}(p_2)\frac{\Gamma_1 \varepsilon_1}{\sqrt{2}}\frac{i}{-\not{q} - m + i\varepsilon}\frac{\Gamma_2 \varepsilon_2}{\sqrt{2}}u(p_1), \tag{5}$$

where ε_1 (ε_2) is the initial (final) polarization vector of the deuteron vertex function Γ_1 (Γ_2). The four-momenta of the incident proton, the outgoing proton, the initial deuteron, final deuteron and exchanged nucleon are p_1, p_2, d_1, d_2 and q, respectively.

Replacing the vertex parts by the nonrelativistic deuteron wave function in the c.m. system, we get

$$M^{l_2 m_2}_{l_1 m_1} = -i2m(q^2-m^2)\times\left[\frac{1}{2m}(32\pi^3 m)^{1/2}\right]^2 \sum_{\alpha}\left\{ C^{1/2\ 1/2\ 1}_{m_1\ l_1-m_2-\alpha\ l_1+1-m_2-\alpha} \times\left[\sum_{L'=0,2} R_{L'}(Q')\, Y^{*}_{L',l_2+m_2-l_1-m_1+\alpha}(\Omega') C^{L'\ 1\ l_2}_{l_2+m_2-l_1-m_1+\alpha\ l_1+m_1-m_2-\alpha} \right] \times C^{1/2\ 1/2\ 1}_{m_2\ l_1-m_2-\alpha\ l_1-\alpha}\left[\sum_{L=0,2} R_L(Q)\, Y_{L\alpha}(\Omega) C^{L\ 1\ l_1}_{\alpha\ l_1-\alpha} \right]\right\}, \tag{6}$$

where $C^{l_1\ l_2\ L}_{m_1\ m_2\ M}$ are Clebsch-Gordan coefficients, the Y_{LM} are spherical harmonic functions, $Q[=\frac{1}{2}(q-p_1)]$ and $Q'[=\frac{1}{2}(q-p_2)]$ are the relative momenta of nucleons inside the initial and final deuteron, and Ω and Ω' are their angles. α is the spin of the internal nucleon. The deuteron wave functions in momentum space, R_L, are related to the D and S wave functions, u and w, as

$$R_0(Q) = \sqrt{\frac{2}{\pi}}\int u(r) j_0(rQ) r\, \mathrm{d}r,$$

$$R_2(Q) = -\sqrt{\frac{2}{\pi}}\int w(r) j_2(rQ) r\, \mathrm{d}r. \tag{7}$$

It is well known that the existence of the D-wave is essential to the tensor analyzing power in the ONE model,

$$T_{20}^{\mathrm{ONE}} = \frac{1}{\sqrt{2}}\frac{(2\sqrt{2}\,R_0 - R_2)R_2}{R_0^2+R_2^2}. \tag{8}$$

2.2. TRIANGLE DIAGRAM

The Feynman amplitude corresponding to fig. 2 is

$$T = \bar{u}(p_2)\int \frac{\mathrm{d}^4 p}{(2\pi)^4}\,\frac{i}{K^2-\mu^2+i\varepsilon}\sqrt{2}\,G\gamma_5\,\frac{i}{\not{n}-m+i\varepsilon}\,\frac{\varepsilon_1 \Gamma}{\sqrt{2}}\,\frac{i}{-\not{p}-m+i\varepsilon}\,\varepsilon_2^{*} A u_1(p_1), \tag{9}$$

where G denotes the pion-nucleon vertex function; p, n, and k are the four-momenta of the internal proton, neutron and pion, and μ is the pion mass. The vertex function A is related to the amplitude for the process $\mathrm{pp}\to\pi^+\mathrm{d}$ by

$$f^{l_2}_{m_1\alpha}(\mathrm{pp}\to\pi\mathrm{d}) = \bar{v}^{(\alpha)}(p)(\varepsilon_2^{(l_2)*}\cdot A)u^{(m_1)}(p_1). \tag{10}$$

There is another diagram which is obtained by interchanging the internal proton and neutron and replacing π^+ by π^0 in fig. 2. This amplitude is related to that of fig. 2 by isospin and is one-half of eq. (9). Therefore the total amplitude is three-halves of eq. (9).

Following Kolybasov and Smorodinskaya [7]), we evaluate eq. (9) in the rest system of the target deuteron and use the nonrelativistic propagator (see appendix (B))

$$\int \mathrm{d}^4p \frac{i}{-\not{p}-m+i\varepsilon} \simeq \int \mathrm{d}^3\boldsymbol{p}\,\mathrm{d}T_\mathrm{p} \frac{-\not{p}+m}{2mT_\mathrm{p}-\boldsymbol{p}^2+i\varepsilon}, \tag{11}$$

where we take the pole term in the integration over the kinetic energy T_p. With the help of the formulae in the appendix (C, D, E) we obtain

$$T^{m_2 l_2}_{m_1 l_1} = \frac{1}{2\sqrt{2\pi^3}} \frac{\sqrt{E_2+m}}{E_2} \sum_{\alpha,\beta} \chi^{(m_2)^\dagger} \boldsymbol{\sigma} \int \mathrm{d}^3\boldsymbol{p} \frac{(\boldsymbol{p}+\tilde{\boldsymbol{p}}_2)+(\boldsymbol{p}'_2-\tilde{\boldsymbol{p}}_2)}{(\boldsymbol{p}+\tilde{\boldsymbol{p}}_2)^2+\delta^2-i\varepsilon} \chi^{(\beta)} G C^{1/2\ 1/2\ 1}_{\alpha\ \beta\ l_1-M}$$
$$\times \left[\sum_L R_L(Q)\, Y_{LM}(\Omega) C^{L\ 1\ l_1}_{M\ l_1-M\ l_1}\right] f^{l_2}_{m_1\alpha}(\mathrm{pp}\to\pi\mathrm{d}), \tag{12}$$

where

$$\boldsymbol{p}'_2 = \frac{E_n+m}{E_2+m}\boldsymbol{p}_2 \simeq \frac{2m}{E_2+m}\boldsymbol{p}_2, \qquad \tilde{\boldsymbol{p}}_2 = \frac{m}{E_2}\boldsymbol{p}_2,$$
$$\delta^2 = \frac{T_2^2}{(1-T_2/m)^2} + \frac{\mu^2}{1-T_2/m}$$

and χ are Pauli spinors. We take f and G out of the integral. To a first approximation we evaluate the energy of $f(\mathrm{pp}\to\pi\mathrm{d})$ in the system where the target proton is at rest. The πNN vertex must be evaluated at the pole of the propagator in the integrand. Using a trick by Kolybasov and Smorodinskaya [7]) (see appendix (F)), the triangle amplitude may be written as

$$T^{m_2 l_2}_{m_1 l_1} = \frac{1}{2\sqrt{2\pi^3}} \frac{\sqrt{E_2+m}}{E_2} G \sum_\alpha f^{l_2}_{m_1\alpha}(\mathrm{pp}\to\pi\mathrm{d})$$
$$\times \chi^{(m_2)^\dagger} \boldsymbol{\sigma} \left(\sum_\beta C^{1/2\ 1/2\ 1}_{\alpha\ \beta\ l_1-M} \chi^{(\beta)}\right) \boldsymbol{B}_{l_1 M}, \tag{13}$$

where

$$\boldsymbol{B}_{l_1 M} = \sqrt{\tfrac{1}{2}\pi} \int \mathrm{d}r\, \mathrm{e}^{i\delta r} \int \mathrm{d}\cos\theta\, \mathrm{d}\phi\, \mathrm{e}^{i\tilde{\boldsymbol{p}}_2\cdot\boldsymbol{r}} \left\{-\frac{\boldsymbol{r}}{r}(r\delta+i) + \frac{\boldsymbol{p}'_2-\tilde{\boldsymbol{p}}_2}{r}\right\}$$
$$\times \sum_L \psi_L(r)\, Y_{LM}(\theta,\phi) C^{L\ 1\ l_1}_{M\ l_1-M\ l_1}. \tag{14}$$

Here ψ_L is the deuteron wave function in r-space,

$$\psi_L(r) = \begin{cases} u(r)/r & (L=0) \\ w(r)/r & (L=2). \end{cases}$$

The angular integration in eq. (14) can be performed explicitly with the help of the formulae in the appendix (G). After a lengthy calculation we finally obtain the

following expression for the triangle diagram amplitudes for the backward pd scattering:

$$a = -CyD_1\,, \qquad c = CvD_1\,,$$
$$b = -CvD_0\,, \qquad c' = -CyD_0\,,$$
$$d = 0\,, \tag{15}$$

where

$$C = \frac{1}{2\sqrt{2\pi^3}}\,\frac{\sqrt{E_2+m}}{E_2}\,G,$$
$$y = -f^1_{\frac{1}{2}\,\frac{1}{2}}(\mathrm{pp}\to\pi\mathrm{d})\,, \qquad v = f^0_{\frac{1}{2}\,-\frac{1}{2}}(\mathrm{pp}\to\pi\mathrm{d})\,,$$
$$D_0 = 2B^{(x)}_{11} - \sqrt{\tfrac{1}{2}}\,B^{(z)}_{00}\,, \qquad D_1 = \sqrt{2}\,B^{(x)}_{11} + B^{(z)}_{10}\,.$$

The amplitudes (15) do not satisfy the constraint from T-invariance, i.e. eq. (4). This is because there is no time-invariance relation in the subprocess $\mathrm{pp}\to\pi\mathrm{d}$. We escape this difficulty as follows. We repeat the above calculation of the triangle diagram in the same way but in the rest frame of the final deuteron. In this case we get the same expression as eq. (15), but c and c' are interchanged. There is no reason to give a preference to one frame or the other, and therefore we average the results obtained in the two final frames:

$$c = c' = \tfrac{1}{2}C(vD_1 - yD_0)\,. \tag{16}$$

3. Results and comparison with the data

For the numerical evaluation of the backward cross section and tensor analyzing power we employed the Reid hard-core wave functions [16]) for the S- and D-state wave functions of the deuteron. The $\mathrm{pp}\to\pi\mathrm{d}$ amplitude $f(\mathrm{pp}\to\pi\mathrm{d})$ was constructed using the partial-wave analysis between threshold and 810 MeV of the Osaka City University group [17]).

The pion–nucleon coupling constant has been well determined in other reactions, and its numerical value is $G^2/4\pi = 14.6$. The results for the backward excitation function are compared with data in fig. 4. The two curves correspond to the two solutions of the partial-wave analysis, called S and D by the Osaka City University group [17]). Both solutions account rather well for the general shape of the bump in the cross section, although the quantitative agreement of the D-solution seems better. The curves stop at $T_\mathrm{p} = 810$ MeV, where the input data for constructing $f(\mathrm{pp}\to\pi\mathrm{d})$ terminate. At the high-energy end of the theoretical calculation both solutions fall with energy more steeply than the experimental data. This fact might suggest that a different subprocess begins to contribute to the backward pd elastic scattering.

The calculation for T_{20} is shown in fig. 5 where data from refs. [14,18]) are reported. Here the S- and D-solutions account for the general trend of the measurements of

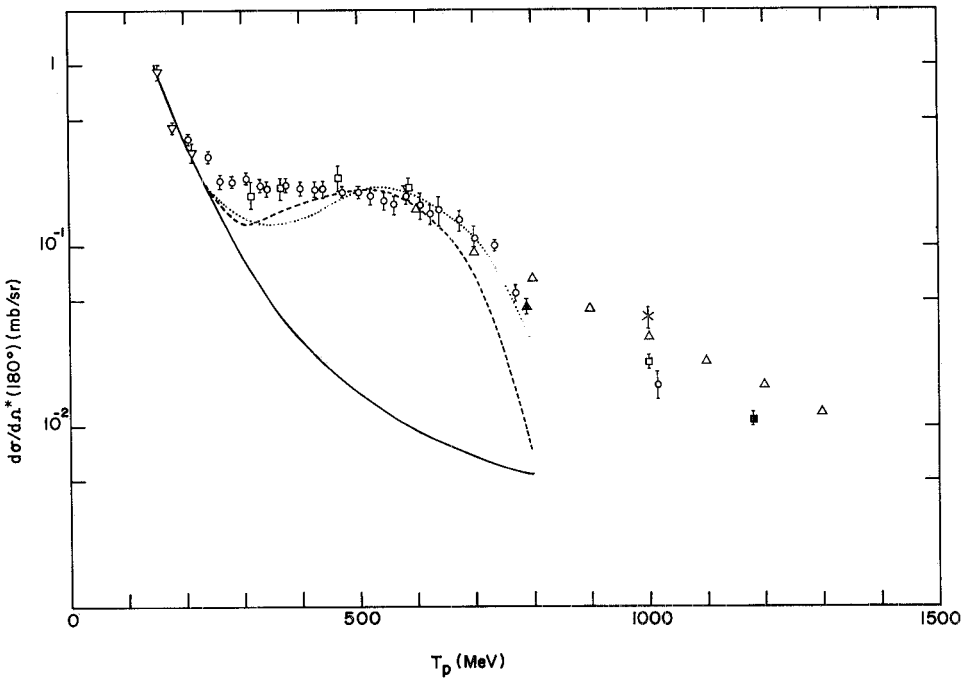

Fig. 4. pd→dp cross section as a function of incident proton kinetic energy. *Solid line*: one-nucleon exchange; *dashed-line*: S-solution of ref. [17]); *dotted line*: D-solution of ref. [17]). Data points are from refs. [1-5]).

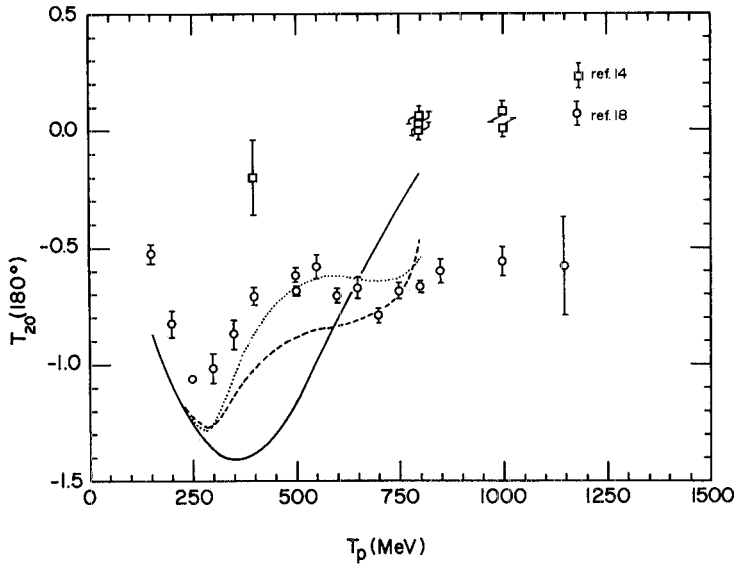

Fig. 5. T_{20} measurements from refs. [14,18]). *Solid line*: one-nucleon exchange; *dashed line*: S-solution of ref. [17]); *dotted line*: D-solution of ref. [17]).

ref. [18]), but the D-solution is clearly favoured. Shape and position of the dip centered at $T_p \simeq 300$ MeV are rather well reproduced. Also the second structure, positioned at $T_p \simeq 700$ MeV, which is stressed by the authors of ref. [18]), is hinted at by the D-solution. It should be pointed out that the rise in T_{20} shown by both solutions towards $T_p = 800$ MeV may be due to the lack of some high angular momentum wave in the partial-wave analysis of ref. [17]).

4. Concluding remarks

We have observed much better agreement between the experimental data and the theory than we had expected. The essential difference between the present calculation and previous ones consists in imposing T-invariance on the triangle amplitudes. Besides this point we have simply tried to write down the spin amplitudes corresponding to figs. 1 and 2. There are, however, still ambiguities in treating the internal momenta. The procedure in the appendix (E) cannot be justified by the Feynman rules.

No parameters appear in the model. In fact we do not need the normalization factor ζ of Barry [8]) which comes from the ambiguity in the internal integral. The only uncertainty comes from two possible solutions of the pp → πd amplitudes. We may use the pd → dp process to supply new information to the pp → πd partial-wave analysis. The T_{20} of pd → dp clearly favors the D-solution. This solution is considered to include two dibaryons $B^2(\text{mass}, J^P) = B^2(2.17, 2^+)$ and $B^2(2.22, 3^-)$ as intermediate states (fig. 6).

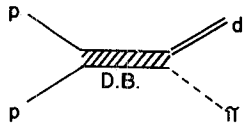

Fig. 6. s-channel dibaryon exchange in the pp → πd reaction.

We have used the pp → πd partial-wave amplitudes. They are expected to be very similar to the real amplitudes and to include many possible mechanisms like the ΔN intermediate state. Therefore our triangle amplitudes automatically include diagrams such as that of fig. 7. Note that the diagram in fig. 7 satisfies T-invariance.

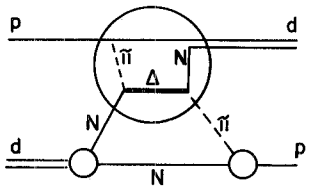

Fig. 7. A possible intermediate mechanism already included in the partial-wave amplitudes employed in the present calculation.

At these energies, however, the ΔN intermediate state is not enough to describe the pp$\to\pi$d amplitude [17,19]). Recently there has been some progress in the analysis of pp$\to\pi$d [refs. [19,20])]. The new analyses include deuteron polarization data, and we are planning to analyze pd$\to$dp using theses new inputs.

We thank W. Watari for sending us the detailed results of the partial-wave analysis of pp$\to\pi$d.

One of the authors (A.N.) is grateful to the hospitality of the theory division at Frascati and CERN, where part of this work was performed. He would also like to thank T. Hasegawa for valuable comments about experimental data, and J. Arafune and Y. Tezuka for helpful discussions.

Appendix

In this appendix some formulae helpful in the evaluation of the amplitudes have been assembled.

A

$$\not{p}+m=2m\sum_{\alpha=1}^{2}u^{(\alpha)}(p)\bar{u}^{(\alpha)}(p)\,,$$

$$-\not{p}+m=-2m\sum_{\alpha=1}^{2}v^{(\alpha)}(p)\bar{v}^{(\alpha)}(p)\,.$$

B

In the rest system of the deuteron (see fig. 1), we have

$$d=(m,\boldsymbol{O})\,,\qquad p=(m+T_{\mathrm{p}},\boldsymbol{p})\,,\qquad q=(m+T_{\mathrm{q}},-\boldsymbol{p})\,,$$

$$T_{\mathrm{p}}\simeq\boldsymbol{p}^2/2m\,,\qquad T_{\mathrm{q}}=m_{\mathrm{d}}-2m-T_{\mathrm{p}}\,,$$

$$p^2-m^2\simeq 2mT_{\mathrm{p}}-\boldsymbol{p}^2\,,$$

$$Q^2-m^2\simeq 2mT_{\mathrm{q}}-\boldsymbol{p}^2=-2(k^2+p^2)\,,$$

where

$$k=\sqrt{m(2m-m_{\mathrm{d}})}\,.$$

C

If the deuteron moves very slowly, its vertex function is related to the nonrelativistic wave function as

$$\bar{u}^{(\beta)}(q)\frac{\varepsilon_1^{(I)}\Gamma}{\sqrt{2}(q^2-m^2)}v^{(\alpha)}(p)=\frac{(32\pi^3m)^{1/2}}{2m}C^{1/2\ 1/2\ 1}_{\alpha\ \beta\ \alpha+\beta}\sum_{L}R_L(Q)\,Y_{LM}(\Omega)C^{L\ 1\ 1}_{m\ \alpha+\beta\ I}\,,$$

where α and β in the Clebsch-Gordan coefficients represent the spins of the states $v^{(\alpha)}$ and $u^{(\beta)}$, respectively, and $\boldsymbol{Q}=\boldsymbol{p}-\frac{1}{2}\boldsymbol{d}\simeq\boldsymbol{p}$.

D

$$\bar{u}^{(l)}(p_2)\gamma_5 u^{(\alpha)}(n) = -\frac{1}{2m}\sqrt{\frac{E_2+m}{E_n+m}}\{\phi^{(l)\dagger}\boldsymbol{\sigma}\cdot(\boldsymbol{p}+\boldsymbol{p}_2')\phi^{(\alpha)}\},$$

where ϕ are Pauli spinors, and

$$\boldsymbol{p}_2' = \frac{E_n+m}{E_2+m}\boldsymbol{p}_2 .$$

In the rest system of the deuteron we may employ the approximation $E_n \simeq m$ in the above formulae.

E

$$p_2 = (m+T, \boldsymbol{p}_2), \qquad n = (m+T, -\boldsymbol{p}).$$

In the rest system of the target deuteron we may replace T_n by T_p. Then we get

$$\begin{aligned} k^2-\mu^2 &\simeq (T_2-T_p)^2-(\boldsymbol{p}_2+\boldsymbol{p})^2-\mu^2 \\ &\simeq \left(1+\frac{T_2}{m}\right)\boldsymbol{p}^2-2\boldsymbol{p}_2\cdot\boldsymbol{p}-2mT_2-\mu^2 \\ &= \left(1+\frac{T_2}{m}\right)[(\boldsymbol{p}+\tilde{\boldsymbol{p}}_2)^2+\delta^2]. \end{aligned}$$

Here $\tilde{\boldsymbol{p}}_2$ and δ are defined in the text.

F

$$\frac{a}{a^2+k^2} = -\frac{i}{4\pi}\int \frac{\boldsymbol{r}}{r}\left(\frac{k}{r}+\frac{1}{r^2}\right)e^{ia\cdot r-kr}\,d^3\boldsymbol{r},$$

$$\frac{1}{a^2+k^2} = \frac{1}{4\pi}\int \frac{1}{r}e^{ia\cdot r-kr}\,d^3\boldsymbol{r}.$$

G

$$e^{ip\cdot r} = 4\pi\sum_l\sum_m i^l j_l(pr)\,Y_{lm}(\theta,\phi)\,Y_{lm}^*(\alpha,\beta).$$

H

$$\int d^3\boldsymbol{p}\, e^{i\boldsymbol{p}\cdot\boldsymbol{r}}R_L(p)\,Y_{LM}(\alpha,\beta) = \begin{cases} \sqrt{4\pi}\sqrt{\frac{1}{2}\pi}\dfrac{u(r)}{r} & (L=0) \\ 4\pi\sqrt{\frac{1}{2}\pi}\dfrac{w(r)}{r}\,Y_{2M}(\alpha,\beta) & (L=2), \end{cases}$$

where we use the formula in part G.

References

1) P. Berthet *et al.*, J. of Phys. **G8** (1982) L111
2) B.E. Bonner *et al.*, Phys. Rev. Lett. **39** (1977) 1253, and references therein
3) L. Dubal *et al.*, Phys. Rev. **9D** (1974) 597
4) J. Banaigs *et al.*, Phys. Lett. **45B** (1973) 535
5) G. Igo *et al.*, Nucl. Phys. **A195** (1972) 33, and references therein
6) N.S. Craigie and C. Wilkin, Nucl. Phys. **B14** (1969) 477
7) V.M. Kolybasov and N.Ya. Smorodinskaya, Phys. Lett. **37B** (1971) 272; Sov. J. Nucl. Phys. **17** (1973) 630
8) G.W. Barry, Ann. of Phys. **73** (1972) 482; Phys. Rev. **D7** (1973) 394
9) J.C. Anjos *et al.*, Nucl. Phys. **A356** (1981) 383
10) S.A. Gurvitz, Phys. Rev. **22C** (1980) 725
11) L.A. Kondratyuk *et al.*, Phys. Lett. **100B** (1981) 448
12) S.S. Vasan, Phys. Rev. **8D** (1973) 4092
13) G. Igo *et al.*, Phys. Rev. Lett. **43** (1979) 425
14) L.A. Kondratyuk and L.U. Schevchenko, Proc. Int. Conf. on high energy nuclear physics, Balatonfured, Hungary 1983, p. 187;
A. Boudard and M. Dilling, Phys. Rev. **31C** (1985) 302
15) J.D. Bjorken and S.D. Drell, Relativistic quantum fields (McGraw-Hill, New York, 1965)
16) R.V. Reid, Ann. of Phys. **50** (1968) 411
17) N. Hiroshige, W. Watari and M. Yonezawa, Prog. Theor. Phys. **68** (1982) 2074
18) J. Arvieux *et al.*, Phys. Rev. Lett. **50** (1983) 19;
J. Arvieux *et al.*, Nucl. Phys. **A431** (1984) 613
19) D.V. Bugg, J. of Phys. **G10** (1984) 47, 717
20) N. Hiroshige, W. Watari and M. Yonezawa, Osaka City University preprint (1984)